Soft Matter

Cite this: *Soft Matter*, 2011, **7**, 11144

www.rsc.org/softmatter

PAPER

Surface immobilized block copolymer micelles with switchable accessibility of hydrophobic pockets†

Julia Gensel,[a] Eva Betthausen,[b] Christoph Hasenöhrl,[a] Katja Trenkenschuh,[a] Markus Hund,[a] Fouzia Boulmedais,[c] Pierre Schaaf,[c] Axel. H. E. Müller[b] and Andreas Fery*[a]

Received 15th July 2011, Accepted 26th September 2011
DOI: 10.1039/c1sm06338c

We report on a novel approach for the design of stimuli-responsive surfaces based on the immobilization of charged ABC triblock terpolymer micelles. The terpolymer consists of a hydrophobic polybutadiene (B) block, a weak anionic poly(methacrylic acid) (MAA) middle block, and a strong cationic end block of quaternized poly(2-(dimethylamino)ethyl methacrylate) (Dq) (BMAADq). In alkaline solutions, this polymer self-assembles into core–shell–corona micelles with a hydrophobic B core, a pH-sensitive MAA/Dq intramicellar interpolyelectrolyte complex (*im*-IPEC) shell, and a cationic corona of excess Dq. These micelles were directly adsorbed onto charged silica as a monolayer creating laterally structured surfaces. The adsorption kinetics was found to follow the theoretical model of random sequential adsorption (RSA). Exposure of the adsorbed micelles to external stimuli (at pH < $pK_{a,apparent}$ of PMAA) induces *im*-IPEC dissolution due to protonation of the MAA block resulting in a changed composition of the shell and both the length and charge density of the corona. Two types of conformational response to pH trigger and therefore, two types of dynamics coupled to short and long relaxation times are involved in the system. The response to pH cycling was shown to be reversible on the short-term scale while the long-term exposure to acidic media causes irreversible changes in the morphology of the micelles as a consequence of the micelles' core mobility and slow rearrangement. In particular, we find that exposure to low pH causes a shape transition to a "doughnut"-like morphology, exposing the core parts of the micelles. In contrast, adsorbed micelles with covalently crosslinked B cores show higher stability to irreversible morphology changes while maintaining the reversible response to pH cycling.

Introduction

The creation of functional surface coatings based on soft matter systems with lateral structure continues to be an attractive research objective in current materials science. Laterally homogeneous surfaces can be obtained by grafting of polymer or polyelectrolyte brushes onto a solid support.[1–3] Alternatively, layer-by-layer deposition of oppositely charged polyelectrolytes allows the formation of laterally homogeneous multilayer films.[4–7] The patterning of these systems can be achieved by additional processes, such as photolithography or micro-contact printing (μCP)[8–10] and selective deposition of polymeric material to pre-patterned surfaces.[11–13]

An alternative approach for laterally structured surfaces is the use of block copolymers by means of spontaneous self-assembly[14–16] or by adsorption of micellar systems.[17–25] The latter case has the advantage to provide regular monolayers of isolated round-shaped particles. Moreover, patterning is possible on the nano-scale, which is difficult to obtain by the methods mentioned above.

One special class of systems used for the preparation of surface coatings is that of stimuli-responsive materials.[26] The interest in such systems originates from the possibility to develop surface coatings for a number of applications[26] including triggerable drug delivery,[27–29] nanoreactors for *in situ* preparation of metal nanoparticles,[18,25,30] and "smart" surfaces.[23,31–34] They show reversible or irreversible response to external stimuli like temperature, pH, ionic strength, or light. In particular after the introduction of stimuli-responsive self-assembly of amphiphilic polystyrene-*block*-poly(acrylic acid) diblock copolymers by Eisenberg and co-workers,[35] stimuli-responsive block copolymer micelles have attracted the attention of many research groups.[36,37]

[a]*Physical Chemistry II, University of Bayreuth, Universitätsstr. 30, 95440 Bayreuth, Germany. E-mail: Andreas.Fery@uni-bayreuth.de*
[b]*Macromolecular Chemistry II, University of Bayreuth, Universitätsstr. 30, 95440 Bayreuth, Germany*
[c]*Institut Charles Sadron, Université de Strasbourg, Centre National de la recherche scientifique, UPR 22, 23 rue du Loess, 67034 Strasbourg Cedex, France*
† Electronic supplementary information (ESI) available. See DOI: 10.1039/c1sm06338c

Generally, block copolymer micelles are dynamic structures and show responsiveness to environmental changes.[38,39] Micellar structures can be "quenched" by covalent crosslinking of the core or shell.[39–41] Another approach to stabilize block copolymer micelles is the reversible ionic complexation of oppositely charged blocks.[42,43] Unlike the covalently crosslinked systems, interpolyelectrolyte complexes (IPECs) can be disassembled by increasing the ionic strength of the solution or, in the case of weak polyelectrolytes, by changes in pH.[44,45] ABC triblock terpolymer micelles,[46,47] having both cationic and anionic blocks, are of specific interest as they can form intramicellar IPECs (*im*-IPECs) without extrinsic crosslinking agents. Recently, Müller and coworkers have reported on dynamic micelles of different triblock terpolymers, which exhibit a core–shell–corona structure with an *im*-IPEC shell.[48–50] The McCormick group introduced the term "self-locked" micelles to clearly distinguish this intramicellar crosslinking process from ionic crosslinking by an extrinsic homopolymer.[51] Very recently, double-layered micellar IPECs were prepared from "self-locked" triblock terpolymer precursor micelles with an *im*-IPEC and a second IPEC with an extrinsic homopolymer resulting in a core–shell–shell–corona structure.[49,52]

Several research groups have studied the adsorption of diblock copolymer micelles onto planar surfaces.[19–21,23,24] The immobilization of stimuli-responsive block copolymer micelles onto solid substrates provides an opportunity to design "smart" surfaces with nano-patterned structure combined with the response to external stimuli, which in solution would lead to aggregation. At the same time, pH-regions that are inaccessible in solution due to colloidal stability issues can be investigated.

Herein, we report on the surface immobilization of stimuli-responsive ABC triblock terpolymer micelles. The terpolymer is composed of a hydrophobic polybutadiene (B) block, a pH-responsive poly(methacrylic acid) (MAA) middle block, and a permanently charged cationic end block of quaternized poly(2-(dimethylamino)ethyl methacrylate) (Dq) (BMAADq). Since the middle block, MAA, is a weak polyacid, the micelles should be pH-sensitive. In alkaline solutions (pH > $pK_{a,apparent}$ of PMAA $\approx$ 5.5), this polymer self-assembles into core–shell–corona micelles with a hydrophobic B core, a MAA/Dq intramicellar interpolyelectrolyte complex (*im*-IPEC) shell, and a cationic corona of uncomplexed Dq. The structure of the micelles in solution was studied by cryogenic transmission electron microscopy (cryo-TEM) and dynamic light scattering (DLS) and is described in detail elsewhere.[50] In the present work, the morphology of a monolayer of adsorbed micelles, their adsorption kinetics on silica as well as the pH response of adsorbed micelles on both short and long-term scales were studied by atomic force microscopy (AFM), scanning electron microscopy (SEM), and quartz crystal microbalance with dissipation monitoring (QCM-D). The slow irreversible response of adsorbed micelles to acidic pH was compared with that of micelles with a covalently crosslinked B core.

Materials and methods

Materials

The triblock terpolymer $B_{800}MAA_{200}Dq_{285}$ (subscripts denoting the degrees of polymerization of the corresponding blocks, $M_n \approx$ 110 000 g mol^{-1}, PDI = 1.10) was synthesized *via* sequential living anionic polymerization in THF followed by polymer-analogous modifications. Details about polymerization and characterization can be found elsewhere.[50] The crosslinking of the micellar B core (x-BMAADq) was performed in aqueous solutions with a UV photoinitiator, Lucirin-TPO (2,4,6-trimethylbenzoylphosphine oxide, BASF), and irradiation with an UV lamp (Hoehnle UVAHAND 250 GS, cut-off at 300 nm).[53,54]

The adsorption experiments were performed with BMAADq micelles at concentrations of 0.11, 0.23, and 0.45 g L^{-1} and with x-BMAADq micelles at a concentration of 0.45 g L^{-1} in commercial pH 10 buffer solutions (AVS Titrinorm from VWR, ionic strength $\approx$ 0.05 M).

Adsorption of BMAADq micelles on solid surfaces

For the adsorption experiments, silicon wafers (CrysTec) with a silica layer of 1.3 nm were used. The silicon substrates were cleaned using the RCA method (sonication in a 1 : 1 mixture of water and 2-propanol for 15 min),[55] followed by heating at 70 °C in a 5 : 1 : 1 mixture of water, 25% ammonia solution, and 30% hydrogen peroxide solution for 10 min. For the QCM-D experiments, QCM sensor crystals (Q-Sense) coated with a ~50 nm thick SiO_2 layer were used.

The triblock terpolymer micelles were adsorbed on freshly cleaned substrates from a 0.45 g L^{-1} BMAADq in pH 10 buffer solution *via* the dip coating method. After one hour the substrate was rinsed with milli-Q water (18.2 MΩ cm) and dried with a stream of nitrogen.

For the kinetic study, Si-wafers were dipped into 0.11, 0.23, and 0.45 g L^{-1} BMAADq in pH 10 buffer solution for controlled periods of time (1–120 min). The substrates were then removed from the solution, rinsed with milli-Q water and dried with nitrogen.

pH treatment of pre-adsorbed micelles

Short-term treatment was performed *in situ* in contact with aqueous solutions of different pH values. For the pH adjustment, HCl and NaOH were used. For the long-term treatment, substrates with pre-adsorbed micelles were immersed into aqueous solutions of pH 4. After treatment, the substrates were intensively rinsed with milli-Q water and dried with nitrogen.

Characterization methods

Atomic force microscopy (AFM) images of dried samples were taken with a commercial AFM (Dimension™ 3100 equipped with a NanoScope® V controller, Veeco Instruments Inc., USA) operating in TappingMode™ using Si_3N_4 cantilevers (OMCL-AC160TS, Olympus) with a typical spring constant of 42 N m^{-1}, a typical resonance frequency of 300 kHz and a tip radius less than 7 nm. For the imaging, light tapping (ratio of set point amplitude to free amplitude ~0.9) was applied. The mean number of adsorbed micelles was determined from at least three images of 5 μm × 5 μm size for each sample using the NanoScope® Analysis software version 1.20. To study the morphology changes of adsorbed micelles after long-term treatment in pH 4, *ex situ* AFM measurements on the same spot of the sample were performed before and after the treatment.

Liquid cell AFM measurements were performed with a Dimension™ 3100 Nanoscope® V operating in Tapping-Mode™. The AFM is equipped with direct drive fluid probe holder (DTFML-DDHE) and cantilevers (SNL-10, Bruker) with a spring constant of 0.24 N m^{-1} were used.

Scanning electron microscopy (SEM) measurements were obtained on a Gemini Leo 1550 instrument operating at 3 keV. Samples were sputtered with a 1.3 nm thin platinum layer.

Cryo-TEM studies were performed on a Zeiss EM922 OMEGA EFTEM instrument according to a standard procedure described before.[49]

The quartz crystal microbalance (QCM-D) measurements were performed on a Q-Sense E1 apparatus from Q-Sense AB (Gothenburg, Sweden) by monitoring the resonance frequencies f and the dissipation factor D of an oscillating quartz crystal upon adsorption of a viscoelastic layer.[56,57] The silicon-coated quartz crystal was excited at its fundamental frequency (5 MHz), and the measurements were performed at the first, third, fifth and seventh overtones, corresponding to 5, 15, 25 and 35 MHz. The QCM measurement is sensitive to the amount of water associated to the adsorbed molecules and senses the viscoelastic changes in the interfacial material.[56] The thickness and the viscosity of the adsorbed layer can be estimated using the viscoelastic Voigt model.[58] For the evaluation, the fluid density (1009 kg m^{-3}), fluid viscosity (0.91 mPa s) and layer density (1000 kg m^{-3}) were kept constant. The thickness was estimated using the 3rd, 5th and 7th overtones. The estimated chi square values for the fitted data are listed in Table S1 (ESI†). Prior to adding the BMAADq solution, the sensor was allowed to equilibrate in pH 4 water and pH 10 buffer solution for 25 and 15 minutes, respectively, to obtain the respective baseline used for the thickness and viscosity evaluation of the adsorbed layer. After the terpolymer micelles injection and signal equilibration, the sensor was rinsed with pH 10 buffer to remove residual polymer, and then, the rinsing water was repeatedly cycled from pH 10 or 7 to pH 4.

Ellipsometry measurements were performed with a Sentech SE 850 spectroscopic ellipsometer at a constant incidence angle of 70°.

Results and discussion

Solution structure

The amphiphilic polymer used in this study is a linear ABC triblock terpolymer consisting of polybutadiene (B), poly(methacrylic acid) (MAA), and quaternized poly(2-(dimethylamino) ethyl methacrylate) (Dq), $B_{800}MAA_{200}Dq_{285}$ (subscripts denoting the degrees of polymerization of the corresponding blocks, $M_n \approx 110\,000$ g mol^{-1}, PDI = 1.10). For simplicity, the polymer will be denoted as BMAADq throughout the manuscript. BMAADq was synthesized *via* sequential living anionic polymerization followed by polymer-analogous modifications as reported before.[50] Its chemical structure is shown in Fig. 1a. In aqueous solutions, BMAADq self-assembles into core–shell–corona micelles with a hydrophobic B core. The solution structure of BMAADq is dependent on pH: at high pH, the attraction between the deprotonated MAA and the positively charged Dq blocks induces the formation of an intramicellar interpolyelectrolyte complex (*im*-IPEC) shell. According to the

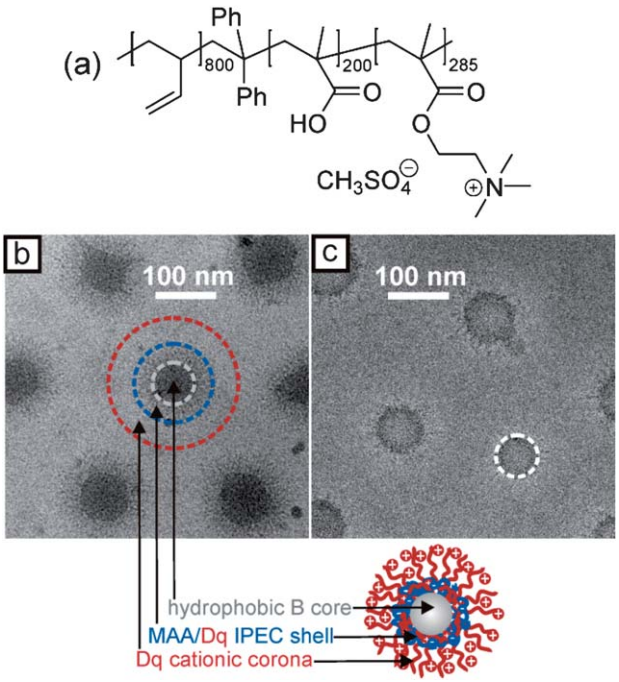

Fig. 1 (a) Chemical structure of the BMAADq terpolymer; (b) 500 nm × 500 nm cryo-TEM micrograph and schematic representation of BMAADq core–shell–corona micelles in alkaline solution (pH 10 buffer). Dashed circles indicate the dimensions of the core (grey) and *im*-IPEC shell (blue) obtained from cryo-TEM and the dimensions of the corona determined by DLS (red). (c) 500 nm × 500 nm cryo-TEM micrograph of BMAADq micelles in acidic solution (pH 4 buffer, dashed circle indicates the dimensions of the core (grey)).

polymerization degrees (DP_n(MAA) < DP_n(Dq)), parts of the cationic Dq block remain uncomplexed forming a positively charged corona. The core–shell–corona structure of the BMAADq micelles was confirmed by cryogenic transmission electron microscopy (cryo-TEM).[50] Fig. 1b shows a cryo-TEM micrograph of the BMAADq micelles at pH 10 with spherical shape and uniform size. The dark hydrophobic B core of 72 nm diameter is surrounded by a 31 nm thick, grey *im*-IPEC shell. The water soluble Dq corona is not visible in the cryo-TEM micrograph due to its low electron density. From dynamic light scattering (DLS) measurements, we obtained a hydrodynamic diameter of the micelles of ~208 nm.[50] The schematic representation of the obtained core–shell–corona micelles is shown in Fig. 1b. Dialysis of BMAADq micelles to low pH (pH 4) results in the formation of a new 11 nm thin dark shell, which could be attributed to collapsed MAA indicating the dissolution of the electrostatic complex between the MAA and Dq (Fig. 1c). Furthermore, the core diameter decreases from 72 to 64 nm while the hydrodynamic diameter increases slightly to ~214 nm.[50]

Surface assembly

For all adsorption experiments, core–shell–corona micelles with *im*-IPEC shell (in pH 10 buffer, Fig. 1b) were used. Due to the positive charge of the Dq corona, one would expect a direct adsorption of the BMAADq micelles onto negatively charged surfaces. Therefore, negatively charged silica was used to

immobilize the triblock terpolymer micelles, which were assembled by dip-coating. The characterization of the adsorbed micelles was carried out by scanning electron microscopy (SEM) and atomic force microscopy (AFM) in the dry state.

Fig. 2a shows a SEM image of dry micelles adsorbed on a Si wafer. The BMAADq micelles form regular arrays of particles with uniform size and spherical-cap shape. The driving force for the surface immobilization is the release of counterions and hydration water upon adsorption.[59,60] The adsorption of coronal chains onto the silica surface inhibits the rearrangement of attached micelles. Electrostatic repulsion between already adsorbed micelles and micelles in solution in conjunction with steric interactions prevents further particle adsorption. As a result, a monolayer of micelles is formed, as often reported for the adsorption behavior of charged soft[19,20,61–63] or rigid colloidal particles.[64,65]

An enlarged SEM image in Fig. 2b shows adsorbed micelles in a dry state with a hydrophobic core (bright) surrounded by an *im*-IPEC shell and a collapsed corona (dark) indicating that the core–shell–corona structure of the triblock terpolymer micelles remains intact upon adsorption to a solid support. The diameter of the micellar core is (78 ± 4) nm based on the average of at least 30 micelles. The average diameter of the adsorbed micelles in the dry state as measured by AFM, corresponding to the diameter of the core and shell, is (124 ± 9) nm and the height is (42 ± 5) nm based on the average of at least 50 micelles. The convolution effect of the tip shape can introduce overestimated lateral dimensions. This effect is of particular relevance for structures having a high aspect ratio and small lateral sizes comparable to the tip radius. However, in our case, the sample features are much larger than the tip radius (Fig. 2c). Therefore, the convolution effect can be neglected.

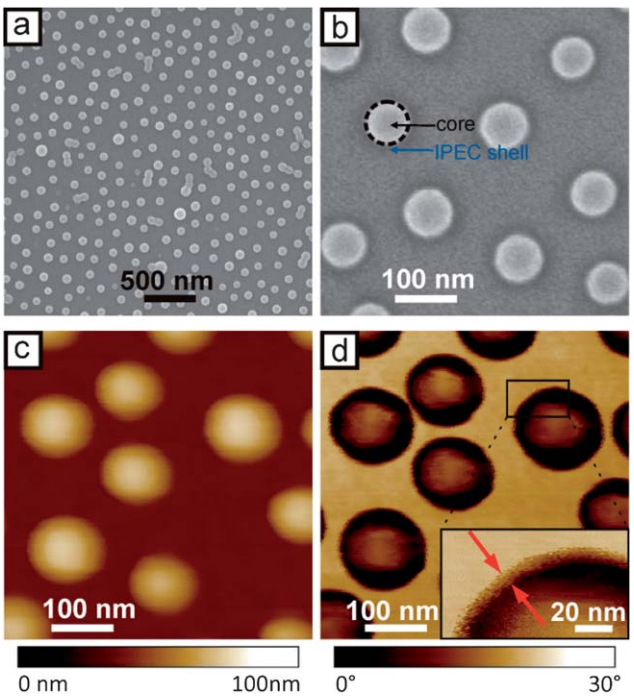

Fig. 2 3 μm × 3 μm SEM image of a monolayer of dry BMAADq micelles adsorbed on a Si wafer (a), 500 nm × 500 nm SEM image of adsorbed micelles with a hydrophobic core (bright, marked by dashed circle) surrounded by an *im*-IPEC shell (dark) (b), 500 nm × 500 nm AFM height (c), and phase image (d) of BMAADq micelles adsorbed on a Si wafer and observed in dry state. Arrows in the enlarged AFM phase image (d, inset) indicate the dimensions of the adsorbed corona.

Compared to the dimensions in solution the core diameter increases slightly upon adsorption and drying while the height decreases. The flattening of the micelles upon adsorption could be explained by a relaxation of attached chains, while the non-adsorbed coronal chains on the top collapse upon drying. Similar flattening of block copolymer micelles due to the relaxation of coronal chains upon adsorption was also reported before.[19,21] The AFM phase image (Fig. 2d, inset) gives additional information about the thickness of the surrounding adsorbed Dq corona, which is 7–8 nm. Including the thickness of the adsorbed corona, which is not detectable in the topography images, the total diameter of the adsorbed micelles is (139 ± 7) nm. Compared to the dimensions in solution, the micellar diameter is decreased and is comparable with the diameter of the micelles in solution excluding the corona (~134 nm).

Due to the additional quantitative analysis of the morphology (phase images), AFM was chosen for further investigations. Moreover, the ability of scanning surfaces in liquids by AFM gives the possibility of monitoring particle response to external stimuli (pH).

Adsorption kinetics

To gain insight into the kinetic aspects of the adsorption process, we used *ex situ* AFM to study the density of adsorbed micelles as a function of time. As the micelles were adsorbed from a buffer solution with an ionic strength of ~0.05 M (Debye length ≈ 1.4 nm), they can be handled as hard spheres due to the screening of the repulsive long-range interactions. Given this and that the micelles adsorb on random locations, we used a method of counting particles adsorbed with cumulative time.[20,61,65]

Fig. 3 shows a series of typical AFM height images of micelles adsorbed from 0.45 g L^{-1} BMAADq solution in pH 10 buffer (ionic strength ≈ 0.05 M). The amount of adsorbed micelles increases rapidly during the first five minutes. At longer adsorption times (15, 30 and 60 minutes), the silica surface appears to become saturated.

The saturation effect of the adsorption process can be shown clearly by plotting the number of adsorbed micelles as a function of the adsorption time. The mean number of micelles was calculated from at least three 5 μm × 5 μm AFM images of BMAADq adsorbed from 0.11, 0.23, and 0.45 g L^{-1} solutions in pH 10 buffer without added salt and is displayed in Fig. 4a. At all three concentrations, the amount of attached micelles increased rapidly in the initial state of adsorption and reached asymptotically the same saturation value.

At the initial adsorption state, micelles that are transported to the surface are not influenced by already adsorbed micelles. Therefore, the adsorption process should be diffusion limited and the number of adsorbed micelles $n_s(t)$ (per unit area) should be proportional to the square root of the adsorption time t according to[66]

$$n_s(t) = 2n_b\sqrt{\frac{D_s t}{\pi}} \quad (1)$$

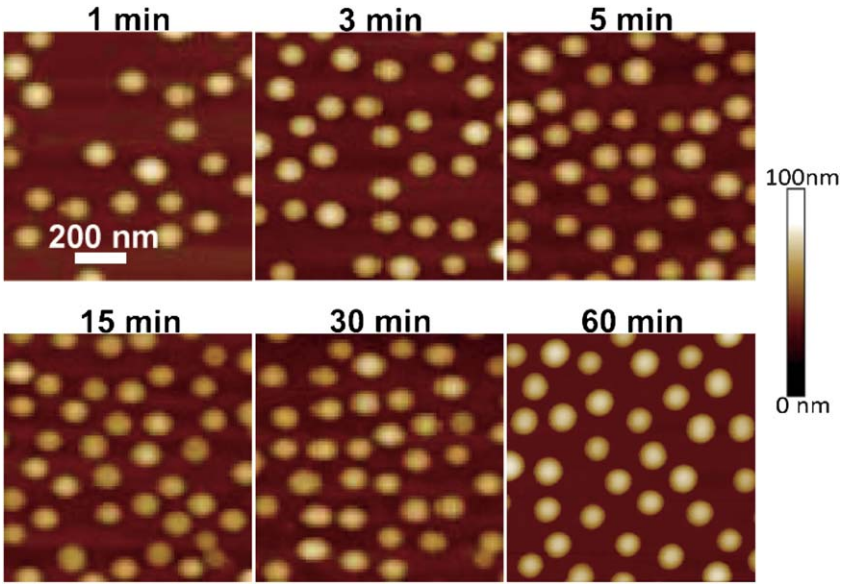

Fig. 3 A series of 1 μm × 1 μm AFM height images of BMAADq micelles adsorbed on Si wafers from 0.45 g L^{-1} solutions in pH 10 buffer without added salt.

where n_b is the number of micelles (per unit volume) in the bulk solution and D_s is the diffusion coefficient of micelles to the silica surface.

A plot of the kinetic data normalized to the number of micelles in solution as a function of the square root of time shows the expected linear relationship at the initial state of adsorption (Fig. 4b). For the three studied concentrations, the slope of the plots in the initial adsorption state is similar, and the mean value of D_s, calculated using eqn (1), is equal to 4.04×10^{-8} cm^2 s^{-1}. The diffusion coefficient D_b of micelles in bulk solution was estimated to be 2.10×10^{-8} cm^2 s^{-1} by DLS. Although different determination methods were used, the experimentally observed initial adsorption rate of BMAADq micelles onto silica is in a reasonable agreement with the diffusion in the bulk solution, which verifies the validity of the diffusion limited regime in the initial adsorption state.

The asymptotical characteristics of micelle adsorption result from surface exclusion effects[67] and have a direct analogy to the theoretical model of random sequential adsorption (RSA) of monodisperse hard spheres.[68,69] The RSA model describes a non-equilibrium process, in which particles are irreversibly attached one by one at random locations on a uniform surface. If the system exhibits RSA kinetics, the surface coverage should asymptotically approach a jamming limit $\theta(\infty)$ according to the relationship[68]

$$\theta(\infty) - \theta(t) \propto t^{-1/2} \quad (2)$$

The surface coverage $\theta(t)$ can be calculated according to the equation $\theta(t) = n_s \pi R_{AFM}^2$, where n_s is the mean number of adsorbed micelles (per unit area) and R_{AFM} is the radius of adsorbed micelles estimated from AFM phase images. Fig. 4c

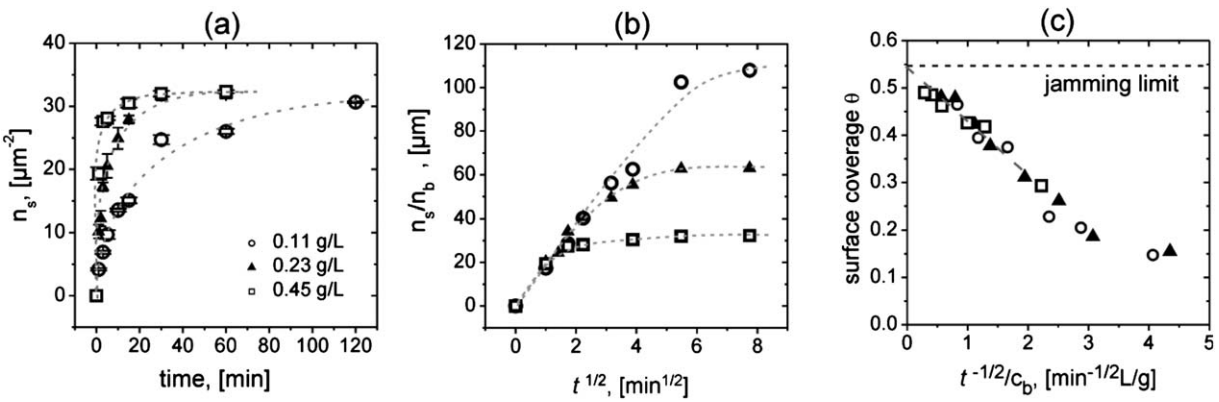

Fig. 4 Mean number of adsorbed micelles, n_s, for different concentrations of BMAADq (0.11 (○), 0.23 (▲), and 0.45 g L^{-1} (□) solutions in pH 10 buffer (ionic strength ≈ 0.05 M)) calculated from *ex situ* AFM measurements as a function of the adsorption time t (a); mean number of adsorbed micelles normalized to the number of micelles in the bulk solution, n_b, *vs.* $t^{1/2}$ (b); surface coverage θ *vs.* $t^{-1/2}$ normalized to the solution bulk concentration c_b (c). Dashed lines are guides to the eye.

shows the surface coverage *vs.* $t^{-1/2}$ normalized to the concentration. For all studied concentrations, the surface coverage scales with $t^{-1/2}$ at longer adsorption times. Extrapolation to the ordinate gives a mean limiting coverage of 0.54 (corresponding to the maximum density of adsorbed micelles $n_{s,max} = 35\ \mu m^{-2}$), which is in a very good agreement with the theoretical jamming limit of 0.547 for the adsorption of monodisperse hard spheres.[70,71]

Stimulus response

BMAADq micelles belong to the class of shell-crosslinked micelles.[41] Unlike covalent crosslinks, ion-pairing like in polyelectrolyte complexes or multilayers can be disassembled by increasing the ionic strength or, in the case of weak polyelectrolytes, by changes in pH.[44,45] Since MAA is a weak polyelectrolyte ($pK_{a,app} \approx 5.5$ (ref. 72)), one would expect changes in the properties and structure of the micelles in response to stimuli like pH and/or ionic strength. Accordingly, the charge density of this block can be adjusted by the pH of the solution.

Reversible stimulus response: short-term effect of pH change

The charge density of the MAA block can be represented by the degree of ionization as a function of pH. In the pH range between 4 and 7, the ionization degree, denoted α, increases from 0 to unity.[73,74] Therefore, we used an *in situ* quartz crystal microbalance with dissipation monitoring (QCM-D) to follow the pH-induced switching of adsorbed micelles in these two extreme cases. The QCM measurement is sensitive to the amount of water associated to the adsorbed micelles and senses the viscoelastic changes in the interfacial material. A decrease in QCM frequency represents as a first approximation an increase in thickness.

Representative data of frequency and dissipation changes for pH cycling are shown in Fig. 5a. After adsorption and rinsing with pH 10 buffer, the adsorbed micelles were rinsed with aqueous solutions of pH above (pH 10 or pH 7) and below (pH 4) the pK_a of the pH-sensitive MAA middle block. The adsorbed micelles show a rapid response to pH cycling. The decrease in the frequency shift at pH 4, *i.e.* increase in thickness, is consistent with the protonation of the MAA block ($\alpha \approx 0$) leading to *im*-IPEC dissolution. Indeed, the uncharged MAA block collapses onto the B core forming a new shell, and the length of the positively charged Dq corona then increases. Longer coronal chains involve swelling of the micelles due to the sorption of additional water and counterions. In conjunction with the decrease in frequency shift, a 6-fold increase in dissipation occurs due to micelles swelling. By increasing the pH to 10, the regeneration of the *im*-IPEC due to the deprotonation of MAA ($\alpha \approx 1$) leads to an increase in frequency shift and a decrease in dissipation. The thickness and the viscosity of the adsorbed layer can be estimated using the viscoelastic Voigt model (Fig. 5b). At pH > pK_a of MAA, the adsorbed micelles exhibit a reduced thickness (55 nm compared to 82 nm) and a higher viscosity as compared to pH 4 respectively due to collapsed Dq corona and to a lower amount of hydration water in the presence of the *im*-IPEC. This short-term response to pH changes is completely reversible after several cycling steps. The disassembly of the *im*-IPEC was also confirmed by cryo-TEM measurements of BMAADq micelles in acidic solutions (Fig. 1c).[50]

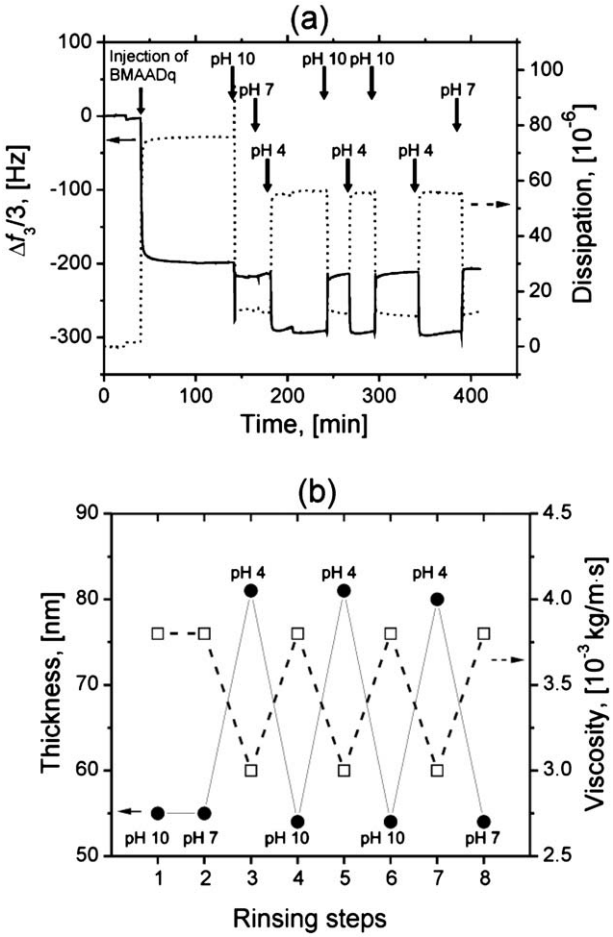

Fig. 5 QCM-D frequency shifts (continuous lines) and dissipation changes (dashed lines), obtained from 15 MHz harmonics (overtone $n = 3$), *versus* time during the adsorption of BMAADq micelles (0.45 g L^{-1} in pH 10 buffer) followed by several rinsing steps with water at different pH values (a); calculated thickness and viscosity, using the viscoelastic Voigt model, of the monolayer of swollen micelles in response to pH cycling (b).

The corresponding AFM images of pre-adsorbed terpolymer micelles in the presence of pH 7 and pH 4 water are shown in Fig. 6a and b respectively. The AFM images strongly correlate with the data observed by QCM-D measurements. Under neutral pH conditions, the height of micelles (43 ± 5) nm is comparable with the height of dry micelles (42 ± 5) nm but smaller compared to QCM data. In contrast, the height of micelles determined by AFM at pH 4 decreased to (27 ± 4) nm (*cf.* cross-sectional height profiles in Fig. 6c) but increased to 82 nm according to QCM. The schematic representation of the topography switching is shown in Fig. 6d. The dissolution of the *im*-IPEC under acidic conditions causes the formation of an uncharged collapsed MAA shell and a long Dq corona, which is penetrable for the AFM tip and therefore not detectable in the topography images in contrast to the QCM that allows determining the hydrodynamic thickness of the micelles, including the Dq corona. Similar observations have been reported in the literature: Hamley *et al.*, for example, performed *in situ* AFM imaging of amphiphilic diblock copolymer micelles observing that AFM is only imaging the core of the micelle rather than the diffuse corona.[24] Similarly, cylindrical

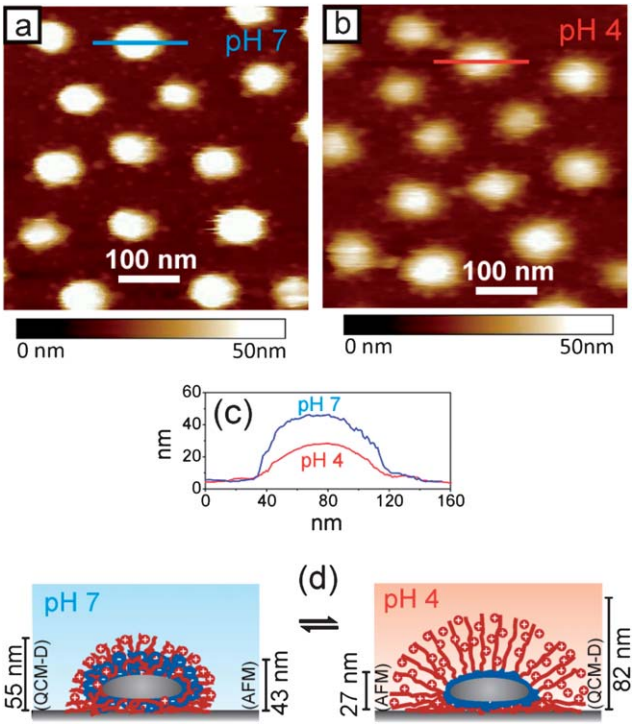

Fig. 6 *In situ* liquid cell AFM height images (500 nm × 500 nm) of pre-adsorbed BMAADq micelles in pH 7 water (a) and pH 4 water (b) with corresponding cross-sectional height profiles (c), and proposed reversible response of an adsorbed BMAADq micelle (d).

brushes with a hard poly(acrylic acid) core and a soft poly(*n*-butyl acrylate) shell only showed the hard core in the height image.[75]

Irreversible stimulus response: long-term effect of pH change

On the one hand, the disassembly of the *im*-IPEC due to the loss of ionic crosslinking in acidic solutions leads to the formation of new interfaces both within the micelle and with water as well as to an increase in the coronal length and charge density. These structural rearrangements are expected to result in changes in the aggregation number of the micelles to minimize the total free energy. The analogous pH decrease from 10 to 4 in the micellar solution leads to a decreased core radius of 32 nm compared to 36 nm at high pH, which might serve as an indication for a dynamic response of the system towards pH change.[50] On the other hand, the desorption process of adsorbed polyelectrolyte chains is entropically unfavourable. This would have two effects: first, the mobility of chains within the micelle should be retarded through entanglements and physically attached chains. Second, the changes in the lateral dimensions of the adsorbed micelles should be hindered. This, together with the strong electrostatic repulsion of coronal chains in the absence of the *im*-IPEC, can induce intramicellar microphase separation of adsorbed micelles if the experimental time is comparable with the longest relaxation time.

The fast pH cycling process discussed in the previous section was shown to be completely reversible as the free energy cannot be minimized on such short-time scales. To gain insight into the

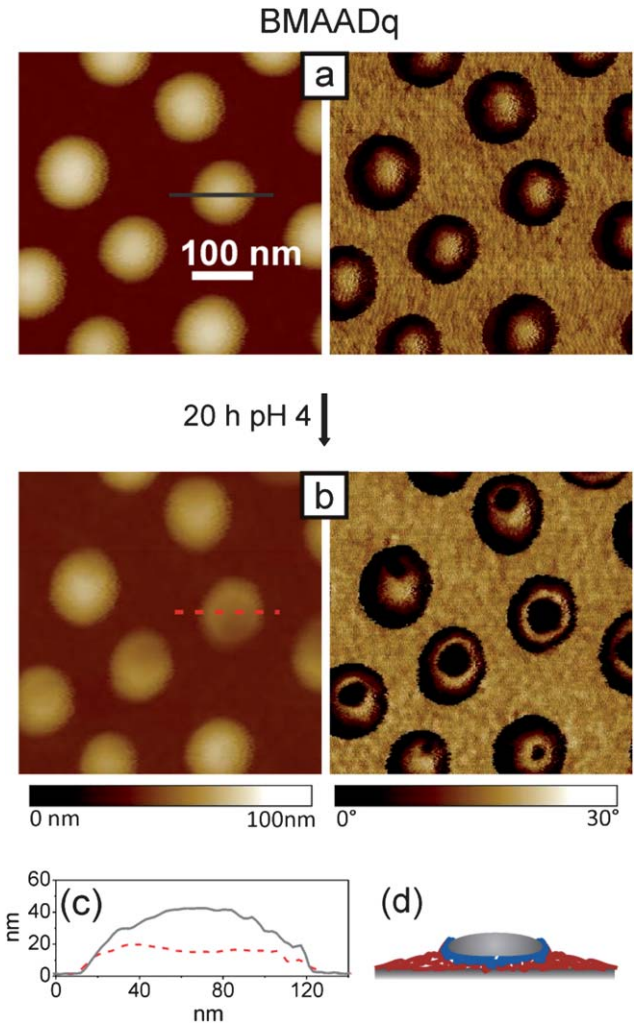

Fig. 7 500 nm × 500 nm AFM height (left) and phase (right) images of dried BMAADq micelles adsorbed on Si-wafers from pH 10 buffer solution (a) and after 20 hours treatment with pH 4 water (b) at the same location of the sample with corresponding cross-sectional height profiles of the same micelle (c) and a schematic representation of observed structure (d).

much slower process of thermodynamic equilibration that involves a change in the aggregation number, we performed long-term treatment of the adsorbed micelles under acidic conditions. The surface morphology was studied *ex situ* by AFM. To precisely follow structural changes of the micelles, we performed measurements on exactly the same spot of the sample before and after the pH treatment and drying. Fig. 7 shows the AFM topography (left) and phase (right) images of the same spot of the sample observed before (Fig. 7a) and after 20 hours contact with pH 4 water (Fig. 7b).

The height image of the adsorbed micelles after long-term treatment in acidic solution (Fig. 7b, left) shows no changes in diameter, but a significant decrease in height from (42 ± 5) nm to (25 ± 6) nm. The measured height profile (Fig. 7c) indicates some deepening towards the middle of the treated micelle, which could be attributed to the deformation of the soft B core by the AFM tip.[76] In contrast, no shape deformation was found for the untreated micelles. Since all measurements were performed in the

same light tapping regime, we conclude that the tip-induced deformation could originate from the formation of an exposed B core. Furthermore, the phase image (Fig. 7b, right) indicates the appearance of a soft material (glass transition temperature T_g(PB) ≈ -28 °C[77]) in the centre of each micelle, the lateral expansion of which corresponds to the size of the core obtained from SEM measurements (Fig. 2b).

The resulting morphological changes may be attributed to the slow surface reorganization of polymer chains that are not electrostatically attached to the surface in order to minimize repulsion of coronal chains. In acidic media, the hydrophobically attached polymer chains within a micelle can dissociate and re-adsorb onto the uncovered silica parts, whereas electrostatically linked chains remain. Since the three blocks are covalently linked, intramicellar microphase separation of adsorbed micelles occurs. After drying and collapse of the MAA shell, the interface of B domains with air can be formed.

To confirm this structural change, we performed ellipsometry measurements. While the morphology of the adsorbed micelles after the long-term treatment at pH 4 changed significantly, the thickness of the sample before and after treatment remains constant (~20 nm) indicating a rearrangement of the micelles on the surface.

Similar irreversible changes have been published by Biggs and co-workers.[21,23,63,78] They have demonstrated the pH-responsive behavior of an on-mica adsorbed monolayer of cationic poly(2-(dimethylamino)ethyl methacrylate)-*block*-poly(2-(diethylamino)ethyl methacrylate) (Dq-DEA) diblock copolymer micelles to pH cycling as a function of the degree of quaternization ($0 < q < 1$) of the D corona.[78] For partly and fully quaternized systems, irreversible changes in the nanomorphology of the adsorbed monolayer were observed after a long-term treatment.[21,78] For non-quaternized systems, however, the close-packed adsorbed micellar layer was found to reversibly open and close the micellar cores in response to solution pH ("nano-anemones").[23,63,78] Interestingly, the same micelles, adsorbed on silica, showed irreversible pH-responsive behaviour upon long-term treatment.[63] In the latter case, the dissociation of micelles on the surface was suggested.

In contrast to these studies, we find microdomain structures with both chemical and topographical patterns of different polarity within domains of round shape on the lateral scale of ~100 nm in ultra-thin films (~20 nm). During submission of this manuscript we became aware of independent work of Tan *et al.* in which similar effects were observed for the systems poly(*N*,*N*-dimethylaminoethyl methacrylate)-*block*-poly(propylene oxide) diblock copolymer micelles and poly(*N*,*N*-dimethylaminoethyl methacrylate)-*block*-poly(propylene oxide)-*block*-poly(*N*,*N*-dimethylaminoethyl methacrylate) triblock copolymer micelles.[79]

Hence, the system provides two relaxation times coupled with the mobility of the B core: fast relaxation in the case of short-term treatment and slow relaxation in the case of irreversible rearrangement of adsorbed micelles. To investigate the role of the core mobility and to support the observed results, we adsorbed micelles with covalently crosslinked B cores (x-BMAADq) onto silica and studied their response to long-term contact with acidic solution. x-BMAADq particles are expected to show a character similar to nanoparticles, the cores of which inhibit any changes in the aggregation number and therefore no reorganization on the surface should be possible.

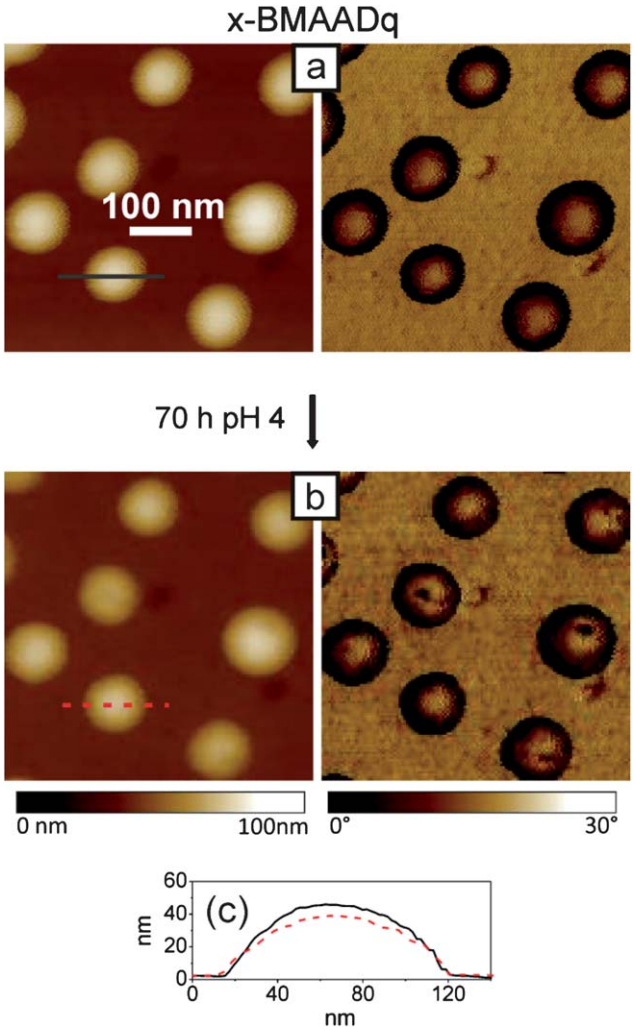

Fig. 8 500 nm × 500 nm AFM height (left) and phase (right) images of dried core-crosslinked x-BMAADq particles adsorbed on Si-wafers from pH 10 buffer solution (a) and after 70 hours treatment with pH 4 water (b) at the same location of the sample, with corresponding cross-sectional height profiles of the same particle (c).

In contrast to BMAADq micelles, almost no topographical and morphological changes occur with x-BMAADq micelles even after 70 hours of pH 4 treatment (Fig. 8). The crosslinking of the core prevents the dynamic behaviour of the micelles and therefore the rearrangement/dissociation of terpolymer chains from adsorbed micelles. The slight decrease in the height of the micelles (Fig. 8c) may be attributed to the relaxation of the corona onto the silica substrate. Since the length of the positively charged corona increases in acidic media, non-adsorbed, mobile Dq chains of adsorbed micelles can adsorb onto uncovered silica. This process is entropically favoured due to the release of hydration water and counterions.[59,60]

Conclusions

The assembly and pH-responsive behaviour of core–shell–corona micelles of a BMAADq triblock terpolymer on silica were

studied. The deposition of micelles onto planar surfaces by a simple dipping method led to well-defined topographical structuring on the nanoscale.

We found that the initial adsorption kinetics of the micelles is determined by the rate of transport to the surface and therefore by the diffusion coefficient, while at later adsorption times, the surface coverage reached a limiting value of 54% consistent with the RSA model.

By controlling the solution pH on the solid–liquid interface of pre-adsorbed micelles, it was possible to reversibly or irreversibly change the micellar morphology and composition. The system involves two types of conformational response to pH trigger and consequently two types of dynamics coupled to the time scales of treatment. On the short-time scale, the pH-responsive behaviour of adsorbed micelles is reversible and can be controlled by the ionization degree of the MAA middle block. The long-term treatment at pH < $pK_{a,apparent}$ of MAA causes changes in the morphology of BMAADq micelles due to the *im*-IPEC dissolution under these conditions and slow micelle reorganization, creating irreversible morphology changes, which are not accessible in solution. This opens interesting opportunities, which will be investigated in further work: while normally the hydrophobic cores are not accessible in aqueous environment, the shape changes observed here indicate an "opening" of the micelles. This makes the micellar cores accessible for chemistry. For example, due to the good stability of such systems in organic solvents, further modifications of the better accessible polybutadiene core *via* click chemistry (*e.g.* thiol–ene reaction) are possible. As well, material (drugs) loaded in the micellar cores is expected to release in the open state.

A further interesting perspective for this system is exploiting the switchable interaction properties. Depending on the swelling state, osmotic pressure due to small counterions confined in the corona is expected to undergo dramatic changes. This results in a change of compressibility of the corona region and/or an expansion which can be used to create volume-work against an external load. Therefore, these systems are potentially interesting as nano-actuators.[79,80] A detailed investigation of these interaction/nano-mechanical properties requires techniques like local force spectroscopy,[81,82] which will be the subject of further investigations. As well, substrates which undergo strong changes in hydration/swelling have been shown to have potential for switchable cell culture substrates.[83] This perspective will as well be explored in further work.

The two relaxation times were found to be linked to the mobility of the B core, as the covalent crosslinking of the core prevents slow irreversible changes, and therefore only one relaxation dynamics was found for the crosslinked system. In contrast to BMAADq, the crosslinked x-BMAADq micelles showed higher stability against morphology changes under long-term acidic conditions, rendering this system of potential interest for long-term experiments *e.g.* drug delivery or the use as switchable surfaces.

Acknowledgements

This research was supported by COST D43 and SFB 840, TP B5. The authors thank Larisa Tsarkova (RWTH Aachen), Georg Papastavrou (University of Bayreuth) and Bernard Senger (INSERM UMR 977, Strasbourg, France) for fruitful discussions. They are also thankful to Nicolas Pazos-Perez (University of Bayreuth) for the help with SEM measurements. E.B. thanks the Bavarian Elite Support Program for a scholarship.

References

1 S. T. Milner, *Science*, 1991, **251**, 905–914.
2 E. B. Zhulina, O. V. Borisov and T. M. Birshtein, *J. Phys. II*, 1992, **2**, 63–74.
3 B. Zhao and W. J. Brittain, *Prog. Polym. Sci.*, 2000, **25**, 677–710.
4 R. K. Iler, *J. Colloid Interface Sci.*, 1966, **21**, 569–594.
5 G. Decher, J. D. Hong and J. Schmitt, *Thin Solid Films*, 1992, **210**, 831–835.
6 G. Decher and J. Schmitt, *Prog. Colloid Polym. Sci.*, 1992, **89**, 160–164.
7 G. Decher, *Science*, 1997, **277**, 1232–1237.
8 A. Kumar and G. M. Whitesides, *Science*, 1994, **263**, 60–62.
9 Y. N. Xia and G. M. Whitesides, *Annu. Rev. Mater. Sci.*, 1998, **28**, 153–184.
10 Y. N. Xia and G. M. Whitesides, *Angew. Chem., Int. Ed.*, 1998, **37**, 551–575.
11 X. P. Jiang and P. T. Hammond, *Langmuir*, 2000, **16**, 8501–8509.
12 X. P. Jiang, H. P. Zheng, S. Gourdin and P. T. Hammond, *Langmuir*, 2002, **18**, 2607–2615.
13 M. Pretzl, A. Schweikart, C. Hanske, A. Chiche, U. Zettl, A. Horn, A. Böker and A. Fery, *Langmuir*, 2008, **24**, 12748–12753.
14 T. L. Morkved, M. Lu, A. M. Urbas, E. E. Ehrichs, H. M. Jaeger, P. Mansky and T. P. Russell, *Science*, 1996, **273**, 931–933.
15 M. Park, C. Harrison, P. M. Chaikin, R. A. Register and D. H. Adamson, *Science*, 1997, **276**, 1401–1404.
16 S. Ludwigs, A. Böker, A. Voronov, N. Rehse, R. Magerle and G. Krausch, *Nat. Mater.*, 2003, **2**, 744–747.
17 J. P. Spatz, T. Herzog, S. Mossmer, P. Ziemann and M. Möller, *Adv. Mater.*, 1999, **11**, 149–153.
18 J. P. Spatz, S. Mossmer, C. Hartmann, M. Möller, T. Herzog, M. Krieger, H. G. Boyen, P. Ziemann and B. Kabius, *Langmuir*, 2000, **16**, 407–415.
19 M. R. Talingting, Y. H. Ma, C. Simmons and S. E. Webber, *Langmuir*, 2000, **16**, 862–865.
20 G. B. Webber, E. J. Wanless, S. P. Armes, F. L. Baines and S. Biggs, *Langmuir*, 2001, **17**, 5551–5561.
21 G. B. Webber, E. J. Wanless, V. Butun, S. P. Armes and S. Biggs, *Nano Lett.*, 2002, **2**, 1307–1313.
22 G. Kästle, H. G. Boyen, F. Weigl, G. Lengl, T. Herzog, P. Ziemann, S. Riethmüller, O. Mayer, C. Hartmann, J. P. Spatz, M. Möller, M. Ozawa, F. Banhart, M. G. Garnier and P. Oelhafen, *Adv. Funct. Mater.*, 2003, **13**, 853–861.
23 G. B. Webber, E. J. Wanless, S. P. Armes, Y. Q. Tang, Y. T. Li and S. Biggs, *Adv. Mater.*, 2004, **16**, 1794–1798.
24 I. W. Hamley, S. D. Connell and S. Collins, *Macromolecules*, 2004, **37**, 5337–5351.
25 J. P. Spatz, T. Lohmueller and E. Bock, *Adv. Mater.*, 2008, **20**, 2297.
26 M. A. Cohen Stuart, W. T. S. Huck, J. Genzer, M. Müller, C. Ober, M. Stamm, G. B. Sukhorukov, I. Szleifer, V. V. Tsukruk, M. Urban, F. Winnik, S. Zauscher, I. Luzinov and S. Minko, *Nat. Mater.*, 2010, **9**, 101–113.
27 T. Addison, O. J. Cayre, S. Biggs, S. P. Armes and D. York, *Langmuir*, 2008, **24**, 13328–13333.
28 Z. C. Zhu and S. A. Sukhishvili, *ACS Nano*, 2009, **3**, 3595–3605.
29 L. Xu, Z. C. Zhu and S. A. Sukhishvili, *Langmuir*, 2011, **27**, 409–415.
30 T. P. Russell, H. D. Koh and S. Park, *ACS Nano*, 2010, **4**, 1124–1130.
31 T. P. Russell, *Science*, 2002, **297**, 964–967.
32 K. Glinel, C. Dejugnat, M. Prevot, B. Schöler, M. Schönhoff and R. V. Klitzing, *Colloids Surf., A*, 2007, **303**, 3–13.
33 P. M. Mendes, *Chem. Soc. Rev.*, 2008, **37**, 2512–2529.
34 M. Stamm, P. Uhlmann, H. Merlitz and J. U. Sommer, *Macromol. Rapid Commun.*, 2009, **30**, 732–740.
35 L. F. Zhang and A. Eisenberg, *Science*, 1995, **268**, 1728–1731.
36 M. Motornov, Y. Roiter, I. Tokarev and S. Minko, *Prog. Polym. Sci.*, 2010, **35**, 174–211.
37 O. J. Cayre, N. Chagneux and S. Biggs, *Soft Matter*, 2011, **7**, 2211–2234.
38 J. Rodriguez-Hernandez, F. Checot, Y. Gnanou and S. Lecommandoux, *Prog. Polym. Sci.*, 2005, **30**, 691–724.

39 R. K. O'Reilly, C. J. Hawker and K. L. Wooley, *Chem. Soc. Rev.*, 2006, **35**, 1068–1083.
40 K. B. Thurmond, T. Kowalewski and K. L. Wooley, *J. Am. Chem. Soc.*, 1996, **118**, 7239–7240.
41 S. P. Armes and E. S. Read, *Chem. Commun.*, 2007, 3021–3035.
42 J. V. M. Weaver, Y. Q. Tang, S. Y. Liu, P. D. Iddon, R. Grigg, N. C. Billingham, S. P. Armes, R. Hunter and S. P. Rannard, *Angew. Chem., Int. Ed.*, 2004, **43**, 1389–1392.
43 M. A. C. Stuart, B. Hofs, I. K. Voets and A. de Keizer, *Curr. Opin. Colloid Interface Sci.*, 2005, **10**, 30–36.
44 V. A. Kabanov, *Russ. Chem. Rev.*, 2005, **74**, 3–20.
45 D. V. Pergushov, Oleg V. Borisov, A. B. Zezin and A. H. E. Müller, *Adv. Polym. Sci.*, 2011, **241**, 131–161.
46 C. A. Fustin, V. Abetz and J. F. Gohy, *Eur. Phys. J. E: Soft Matter Biol. Phys.*, 2005, **16**, 291–302.
47 J. F. Gohy, N. Willet, S. Varshney, J. X. Zhang and R. Jerome, *Angew. Chem., Int. Ed.*, 2001, **40**, 3214–3216.
48 F. Schacher, A. Walther and A. H. E. Müller, *Langmuir*, 2009, **25**, 10962–10969.
49 F. Schacher, E. Betthausen, A. Walther, H. Schmalz, D. V. Pergushov and A. H. E. Müller, *ACS Nano*, 2009, **3**, 2095–2102.
50 E. Betthausen, M. Drechsler, M. Förtsch, F. H. Schacher and A. H. E. Müller, *Soft Matter*, 2011, **7**, 8880–8891.
51 C. L. McCormick, J. D. Flores, X. W. Xu and N. J. Treat, *Macromolecules*, 2009, **42**, 4941–4945.
52 F. H. Schacher, C. V. Synatschke, M. Förtsch, M. Drechsler and A. H. E. Müller, *Soft Matter*, 2011, **7**, 1714–1725.
53 A. Walther, A. S. Goldmann, R. S. Yelamanchili, M. Drechsler, H. Schmalz, A. Eisenberg and A. H. E. Müller, *Macromolecules*, 2008, **41**, 3254–3260.
54 E. Betthausen, F. Schacher and A. H. E. Müller, in preparation.
55 W. Kern and D. A. Puotinen, *RCA Rev.*, 1970, **31**, 187–206.
56 K. A. Marx, *Biomacromolecules*, 2003, **4**, 1099–1120.
57 F. Hook, J. Voros, M. Rodahl, R. Kurrat, P. Boni, J. J. Ramsden, M. Textor, N. D. Spencer, P. Tengvall, J. Gold and B. Kasemo, *Colloids Surf., B*, 2002, **24**, 155–170.
58 M. V. Voinova, M. Rodahl, M. Jonson and B. Kasemo, *Phys. Scr.*, 1999, **59**, 391–396.
59 C. B. Bucur, Z. Sui and J. B. Schlenoff, *J. Am. Chem. Soc.*, 2006, **128**, 13690–13691.
60 J. B. Schlenoff, A. H. Rmaile and C. B. Bucur, *J. Am. Chem. Soc.*, 2008, **130**, 13589–13597.
61 R. Pericet-Camara, G. Papastavrou and M. Borkovec, *Langmuir*, 2004, **20**, 3264–3270.
62 R. Pericet-Camara, B. P. Cahill, G. Papastavrou and M. Borkovec, *Chem. Commun.*, 2007, 266–268.
63 K. Sakai, E. G. Smith, G. B. Webber, M. Baker, E. J. Wanless, V. Bütün, S. P. Armes and S. Biggs, *Langmuir*, 2006, **22**, 8435–8442.
64 Z. Adamczyk, M. Zembala, B. Siwek and P. Warszynski, *J. Colloid Interface Sci.*, 1990, **140**, 123–137.
65 C. A. Johnson and A. M. Lenhoff, *J. Colloid Interface Sci.*, 1996, **179**, 587–599.
66 H. Motschmann, M. Stamm and C. Toprakcioglu, *Macromolecules*, 1991, **24**, 3681–3688.
67 P. Schaaf and J. Talbot, *J. Chem. Phys.*, 1989, **91**, 4401–4409.
68 Y. Pomeau, *J. Phys. A: Math. Gen.*, 1980, **13**, L193–L196.
69 P. Schaaf, J. C. Voegel and B. Senger, *J. Phys. Chem. B*, 2000, **104**, 2204–2214.
70 J. Feder, *J. Theor. Biol.*, 1980, **87**, 237–254.
71 E. L. Hinrichsen, J. Feder and T. Jossang, *J. Stat. Phys.*, 1986, **44**, 793–827.
72 H. Dautzenberg, W. Jaeger, J. Kötz, B. Philipp, C. Seidel and D. Stscherbina, *Polyelectrolytes*, Carl Hanser Verlag, München, 1994.
73 I. Borukhov, D. Andelman, R. Borrega, M. Cloitre, L. Leibler and H. Orland, *J. Phys. Chem. B*, 2000, **104**, 11027–11034.
74 G. Battaglia, C. Fernyhough and A. J. Ryan, *Soft Matter*, 2009, **5**, 1674–1682.
75 M. F. Zhang, T. Breiner, H. Mori and A. H. E. Müller, *Polymer*, 2003, **44**, 1449–1458.
76 J. Tamayo and R. Garcia, *Langmuir*, 1996, **12**, 4430–4435.
77 W. A. Lee and R. A. Rutherford, *Polymer Handbook*, John Wiley and Sons, New York, 2nd edn, 1975.
78 G. B. Webber, E. J. Wanless, S. P. Armes and S. Biggs, *Faraday Discuss.*, 2005, **128**, 193–209.
79 W. S. Tan, Z. Zhu, S. A. Sukhishvili, M. F. Rubner and R. E. Cohen, *Macromolecules*, 2011, **44**, 7767–7774.
80 W. S. Tan, R. E. Cohen, M. F. Rubner and S. A. Sukhishvili, *Macromolecules*, 2010, **43**, 1950–1957.
81 V. V. Tsukruk, A. Sidorenko, V. V. Gorbunov and S. A. Chizhik, *Langmuir*, 2001, **17**, 6715–6719.
82 P. A. L. Fernandes, S. Schmidt, M. Zeiser, A. Fery and T. Hellweg, *Soft Matter*, 2010, **6**, 3455–3458.
83 S. Schmidt, M. Zeiser, T. Hellweg, C. Duschl, A. Fery and H. Möhwald, *Adv. Funct. Mater.*, 2010, **20**, 3235–3243.